

FLUIDIZATION PROPERTIES OF COAL CHAR

Herman F. Feldmann, Koh-Don Kiang, and Paul M. Yavorsky

Pittsburgh Energy Research Center, U. S. Department of the Interior,
Bureau of Mines, 4800 Forbes Avenue, Pittsburgh, Pa. 15213

INTRODUCTION

Coal reserves are vast and therefore will play an ever-increasing role in supplying our growing energy demands. However, because of predicted shortages of liquid and gaseous fuels and because of environmental considerations, future utilization will include the development of processes to desulfurize coal as well as to convert it to liquid and gaseous fuels that would also be desulfurized.

Thus, processes such as pyrolysis, desulfurization, gasification, hydrogasification, carbonization, as well as fluid-bed combustion, are being developed to allow coal to broaden its role in satisfying future energy and chemical demands. These processes have at least two features in common: First, they will likely utilize char, derived from coal, as a feed or a constituent in some reactor zone. Second, as a corollary of the particulate nature of char, the processes can use fluidized-bed reactors to take advantage of the improved heat and mass transfers, easier flow operations, good mixing, and ease of control. The design of reactor systems to carry out the above processes therefore requires knowledge of the fluidization properties of coal chars, as well as knowledge of reaction thermodynamics and kinetics.

This study was made to provide the necessary fluidization data for the design of fluid-bed hydrogasifiers of both laboratory and commercial scale. An excellent summarization of fluidization data for various materials appears in the literature.¹ Additional data on chars are also available.^{2,3} However, the char we will be fluidizing is so different that use of the published data is precluded. The correlations presented here should allow extension of data to the design of any other fluid-bed reactor system using coal chars that have the same physical characteristics. Apparently, no universal correlation has been developed to account perfectly for all the physical parameters involved in fluidization; thus, no single correlation now exists that suits all particulate materials regardless of constitution or especially particle shape. Separate correlations still appear to be needed for widely varied materials, as will be demonstrated here. The particular char used in these experiments was produced by rapid hydrogasification of raw high-volatile bituminous coal in a "free-fall" reactor. In our overall process concept to produce pipeline gas from coal, this lightly converted char (25 to 30 percent carbon conversion) would fall into a fluid-bed reactor for additional carbon conversion and for the removal of sufficient hydrogasification heat to maintain the reaction temperature at 1,600° to 1,700° F. The free-fall reactor system has been analyzed⁴ and an integrated reactor system is now being designed to add a fluid-bed reactor below this dilute phase to allow both an experimental and an engineering evaluation of the overall process thus integrated.

EXPERIMENTAL

Material. The char used in this study was produced by concurrent injection of raw bituminous coal and hot hydrogen:methane (1:1) mixture into the top of a 5 ft x 3 in. id reactor at 1,000 psig and 1,650° F. Very rapid devolatilization, gasification of the volatiles, and partial hydrogasification of char all occur. The resultant char falls freely in the slowly down-flowing gas. Carbon conversion in the above reactor is from 25 to 30 percent.

Apparatus. The fluidization studies were conducted at atmospheric pressure with the majority of the tests in a plexiglass column of 3.69-inch id. The fluidizing gas was introduced at the bottom of the column through a porous sintered stainless steel distributor plate, 1/4 inch thick with an average pore size of 5 microns. Thinner, more porous distributors were avoided when found to induce more channeling in the fluid bed, especially at the reactor bottom. The bed depth was varied from almost 3 feet to a few inches with no appreciable change in fluidization properties. Two experiments were made in a two-inch id tube with static heights of approximately five feet to observe the fluidization behavior of this char at conditions anticipated for a bench-scale fluidized-bed char hydrogasifier. Gas rates and pressure drops were measured with the usual rotameters and manometers.

RESULTS

Char Properties. A char property important to fluidization is the effective particle density. Because of the sudden heating in the dilute-phase hydrogasifier as described above, this char has a very large fraction of internal void space so that the density is much less than that of the feed coal or chars from slow carbonization. A photomicrograph of a typical char particle is shown in figure 1 to illustrate the internal structure of this char.

Because of the vesicularity of this char, the effective density of the char particles is not known directly, but can be calculated from bulk density and gas-flow pressure drop measurements made on packed beds according to the procedure recommended by Leva⁵ using Ergun's correlations.⁶

As shown in figure 2, the particle densities measured in the above manner fall into two categories, depending on the particle diameter. For fine particles where $\bar{d}_p < .003$ in., the effective particle density is about 26 lb/cu ft while for the coarser particles where $\bar{d}_p > .01$ in., the particle density is about 16 lb/cu ft. For $.003 < \bar{d}_p < .01$ there seems to be a transitional region, although only one data point is included in this particle size range. The most likely explanation of this behavior is that below a certain particle diameter, the particles cannot be vesicular and therefore must have a higher effective solid density than larger particles which can contain many vesicles. This explanation is consistent with the microphotograph shown in figure 1 because the approximate size range of the vesicles is about equal to the particle diameter at which the density transition occurs. Therefore, because the vesicles seem to have a limiting minimum size, particles smaller than this minimum size are nonvesicular. Physical interpretation of this effect is possible. Volatile matter evolved inside small particles of rapidly heated coal can escape without forming a vesicle because of the shorter diffusional path, or because any "skin" of coal in its plastic phase is too thin and bursts before a sizable vesicle can form. The larger particles can have thicker, stronger plastic layers to contain the evolved volatile matter long enough to make vesicles, and the diffusional escape of gas is, of course, more restrained.

The bulk density dependence on mean particle size is shown in figure 3. The mean particle diameter is here defined, as recommended by Leva⁴, by $\frac{1}{\bar{d}_p} = \frac{\sum X_i}{d_{pi}}$. The

discontinuity of bulk density versus size occurs at the same particle diameter as was observed for the discontinuity of particle density versus size. However, the bulk density curve for the vesicular particles is slightly above the curve for the nonvesicular particles in spite of the higher solid density of the nonvesicular particles. The most likely explanation for this experimental observation is that the wider variety of particle shapes one finds in the larger particle size mixtures permits closer packing which more than compensates for the decreased solid density.

The smaller sized particles, being more spherical, apparently pack with a higher void space, causing a decrease in the bulk density.

Minimum Fluidization Velocity. The minimum fluidization velocity was found to depend on the properties of the solid and fluid in a way that permits use of the dimensionless Galileo number, N_{Ga} for correlation. A correlation that empirically fits the data was obtained by plotting $\log(N_{Re})$ against $\log(N_{Ga})$, as suggested by Wen and Yu.¹ The resulting correlation is shown in figure 4. An excellent straight line results for both narrow and wide particle size distributions when the mean particle diameter as defined above is used.

Some other salient features of the correlation presented in figure 4 are:

(1) Though self-consistent, our correlation using mean particle sizes does not agree with that of Wen and Yu.¹ (2) For narrow size distributions, as expected, it does not make much difference whether mean or maximum particle size is used; a self-consistent correlation occurs either way. (3) For the few points available for broad size distributions, attempted correlation is poor when maximum particle size, as recommended by Wen and Yu, is used instead of mean particle size.

In view of the above three features, it is recommended that average particle diameters be used with our correlation for predictive purposes with similar chars.

In general, the chars used in these studies require much larger velocities to fluidize than predicted by reference 1. The difference between the correlations is too great to attribute to inaccuracies in measuring ρ_s , which is the least accurate term in the Galileo number. Examination of the char particles reveals the most likely reason for the deviation between correlations is the configuration or shape of the respective particles. A picture of some typical char particles in figure 5 shows that the "particles" consist of a sizable fraction of agglomerates of small particles and that these agglomerates can readily interlock. Thus, collisions between particles in the fluid bed will frequently result in the particles catching together which results, momentarily, in an increase in the effective particle diameter in the bed and the requirement of additional energy to move the combination or to unhook the particles. Because this additional energy can only be supplied through increased gas velocity, these particles fluidize at higher velocities than particles having identical properties except for less ability to interlock upon collision. In deciding whether to use the correlation based on these results or that based on more "regular" particles, it would probably be sufficient to examine the particles to see whether they contain shapes that can cause them to hook together and thereby require the use of higher fluidization velocities.

A summary of the fluidization data is given in table 1 to illustrate the range of particle sizes and bed heights used to derive the correlation in figure 4. The minimum fluidization velocity was obtained in the classical manner by plotting the experimentally measured bed pressure drop against the gas velocity, and defining the velocity at which ΔP just reaches $\Delta P = \frac{W_b}{A_T}$ as the minimum fluidization velocity.

A typical ΔP vs u curve is shown in figure 6a for a relatively narrow particle size range.

In general, fluidization was visibly smoother for narrow size fractions of particles. However, wide fractions of only coarser particles also behaved well. The most irregular fluidization was experienced with wide size fractions having appreciable concentrations of fine particles, leading to behavior illustrated in figure 6b,

TABLE 1. - Summary of fluidization data for coal char fluidized with CO₂; tube id = 3.69 (with exceptions noted below)

Particle size range, U. S. Sieve Series	Mean particle diameter, in.	Minimum fluidization velocity, ft/sec	Reynold's No. at minimum fluidization	Galileo number	Bed height at minimum fluidization, in.	Wt of char in bed, lb
6 X 8	0.113	1.42	151	3.6 X 10 ⁵	9.0	0.248
8 X 12	0.08	1.06	80	1.2 X 10 ⁵	11.0	0.339
12 X 14	0.061	0.74	43	6.24 X 10 ⁴	8.2	0.280
14 X 20	0.044	0.57	23.8	2.5 X 10 ⁴	10.8	0.410
20 X 40	0.025	0.37	8.8	5.15 X 10 ³	10.6	0.480
40 X 60	0.013	0.14	1.8	810	3.7	0.209
60 X 80	0.0084	0.11	0.87	254	2.6	0.183
80 X 120	0.0059	0.085	0.48	101	2.0	0.163
120 X 200	0.0039	0.059	0.21	28.6	11.6	0.789
200 X 325	0.0022	0.040	0.080	6.02	13.0	1.51
1/6 X 40	0.065	1.23	75	1.34 X 10 ⁵	24.0	0.546
1/6 X 40	0.071	1.27	85	1.57 X 10 ⁵	30.0	0.825
1.2/100% -14,						
34% -325	0.0052	0.05	0.25	61	47.0	1.0
1.2,3/100% -14,						
34% -325	0.0052	0.03	0.076	26	47.0	1.0

1/ Data given by solid points on figure 4.

2/ Tube id = 2 inches.

3/ Fluidized with N₂.

where precise definition of U_{mf} was difficult. Appreciable channelling and segregation was noted with the particle size range illustrated in figure 6b, but this could be overcome by going to velocities considerably higher than U_{mf} where performance stabilized even with the relatively high L/D ratio used in this test.

Design Considerations. To design a fluid-bed chemical reactor, it is generally not sufficient to know only U_{mf} because one must operate at a velocity sufficient to give vigorous mixing and prevent the segregation of particles. With the narrow particle size ranges, it was found that a gas velocity twice that of U_{mf} was sufficient to provide good mixing and to prevent segregation. However, as mentioned above, for the wide particle size distribution (100 percent -14 to 34 percent -325) in table 1, it was necessary to operate at $U/U_{mf} > 7$ before complete mixing was achieved.

To calculate the mean solids residence time in a fluid-bed reactor requires knowing the amount of bed expansion as a function of operating conditions. The data below indicate that the expansion ratio depends on the mean particle size as well as U/U_{mf} . A summary of experimental results is shown in figure 7a and 7b where L/L_{mf} is plotted against U/U_{mf} for various particle sizes. As the mean particle size decreases, so does the bed expansion ratio for a fixed U/U_{mf} until d_p reaches about 0.025 in., below which further reductions in particle size do not change the expansion behavior. For wide particle size ranges, the previously defined mean diameter determines the bed expansion as is indicated in figure 7b where expansion ratios for fluid beds having char particles from 14 to 325 mesh are plotted. Also in figure 7b, data are shown for narrower particle size distribution tests made with particle diameters below .025 inch.

CONCLUSIONS

The minimum fluidization velocity of coal chars, physically similar to those studied here, can be predicted for various particle sizes and gas conditions by computing the Galileo number and fitting it to the correlation developed here. To get the Galileo number requires knowledge of mean particle size, particle density, and gas density and viscosity at conditions for the desired system. The correlation applies to both narrow and wide particle size distributions and over a range of "Reynolds numbers at minimum fluidization" from less than 0.1 to over 100. The minimum fluidization velocity predicted by our experimental correlation is considerably higher than one would calculate from existing theory and from other correlations because of small agglomerates in the char which cause entanglement and thus require an additional energy input to either separate them or fluidize the more massive combination. Correlations are also presented for fluid-bed expansion that indicate that the mean particle size is the main factor in determining how bed expansion will vary with gas velocity.

NOTATION

U = superficial gas velocity, ft/sec

U_{mf} = superficial gas velocity, at minimum fluidization, ft/sec

ρ_f = density of fluid phase, lb/cu ft

ρ_s = effective density of solid phase, lb/cu ft

ρ_b = bulk density of bed, lb/cu ft

d_{pi} = particle diameter, ft

X_i = weight fraction of particles having diameter d_{pi}

d_p = mean particle diameter, ft

μ = gas viscosity, lb/ft-sec

W_s = weight of solid in bed, lb

A_T = cross sectional area of tube, sq ft

ΔP = pressure drop across bed, lb/sq ft

L = bed height, ft

L_{mf} = bed height at minimum fluidization, ft

D_T = tube diameter, ft

g = acceleration of gravity, ft/sec²

N_{Ga} = Galileo number = $d_p \rho_f (\rho_s - \rho_f) g \mu^{-2}$

(N_{Re}) = Reynold's number at minimum fluidization

$$= d_p U_{mf} \rho_f \mu^{-1}$$

REFERENCES

1. Wen, C. Y. and Y. H. Yu. Chem. Eng. Prog. Symposium Series, v. 62, No. 62, 1966, pp. 100-111.
2. Jones, J. F., R. T. Eddinger, and L. Seglin. Proceedings of International Symposium on Fluidization, Eindhoven Netherlands, N.U.P. Amsterdam, June 6-9, 1967, published by Netherlands University, Amsterdam.
3. Curran, G. P., and Everett Gorin. Studies on Mechanics of Fluo-Solids Systems. Period July 1964 to June 1968, R & D Report No. 16, Interim Report No. 3, Book 1, OCR Contract 14-01-0001-415, Consolidation Coal Co., Research Division, Library, Pa.
4. Feldmann, H. F., W. H. Simons, J. A. Mima, and R. W. Hiteshue. ACS Div. of Fuel Chem. Preprints, v. 14, No. 4, Part II, pp. 1-13, Sept. 1970.
5. Leva, Max. Fluidization, McGraw Hill Book Co., Inc., N. Y. 1959, pp. 60, 61.
6. Ergun, Sabri. Anal. Chem., v. 24(2):388 (1952).

ACKNOWLEDGEMENTS

The help of Mr. David A. Williams and Mr. Joseph A. Mima in conducting the experiments and the helpful advice of Dr. C. Y. Wen are gratefully acknowledged.



FIGURE 1.- Cross Section of Typical Char Particle
at 220 Magnification.

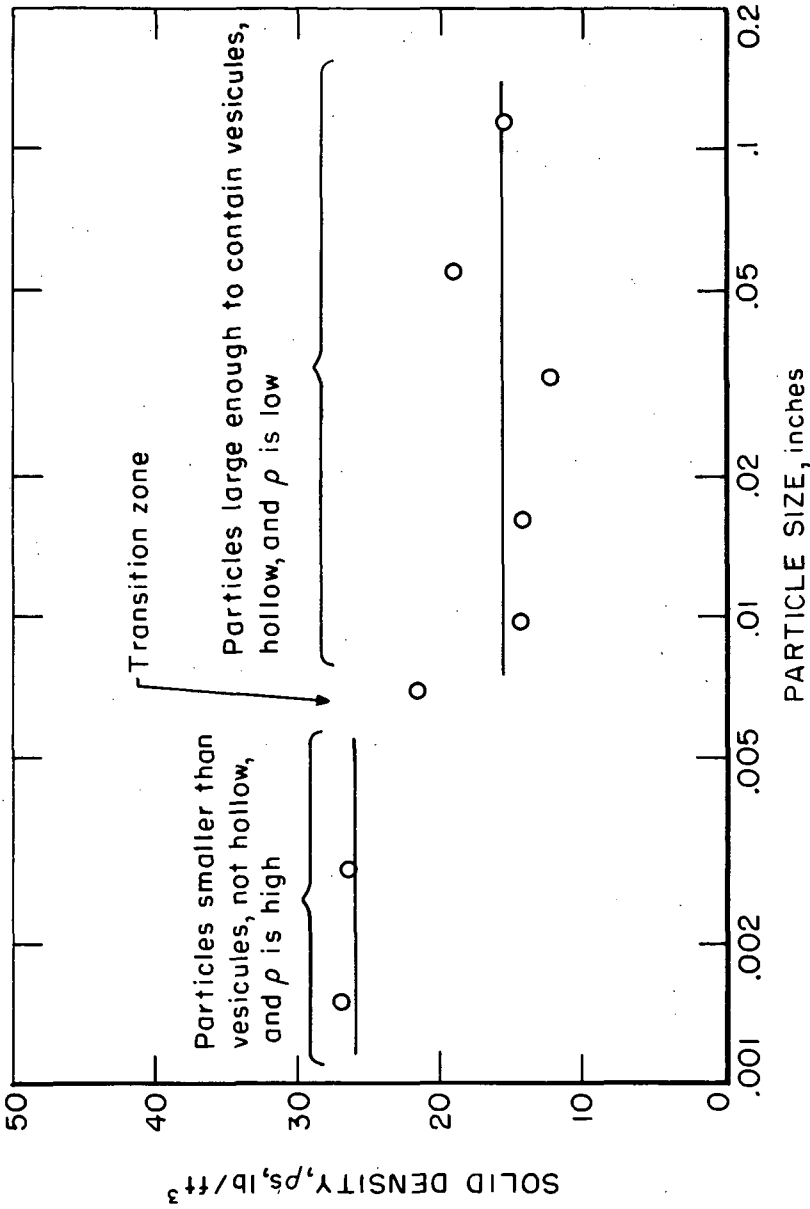


FIGURE 2.- Particle Density vs Particle Size of Char.

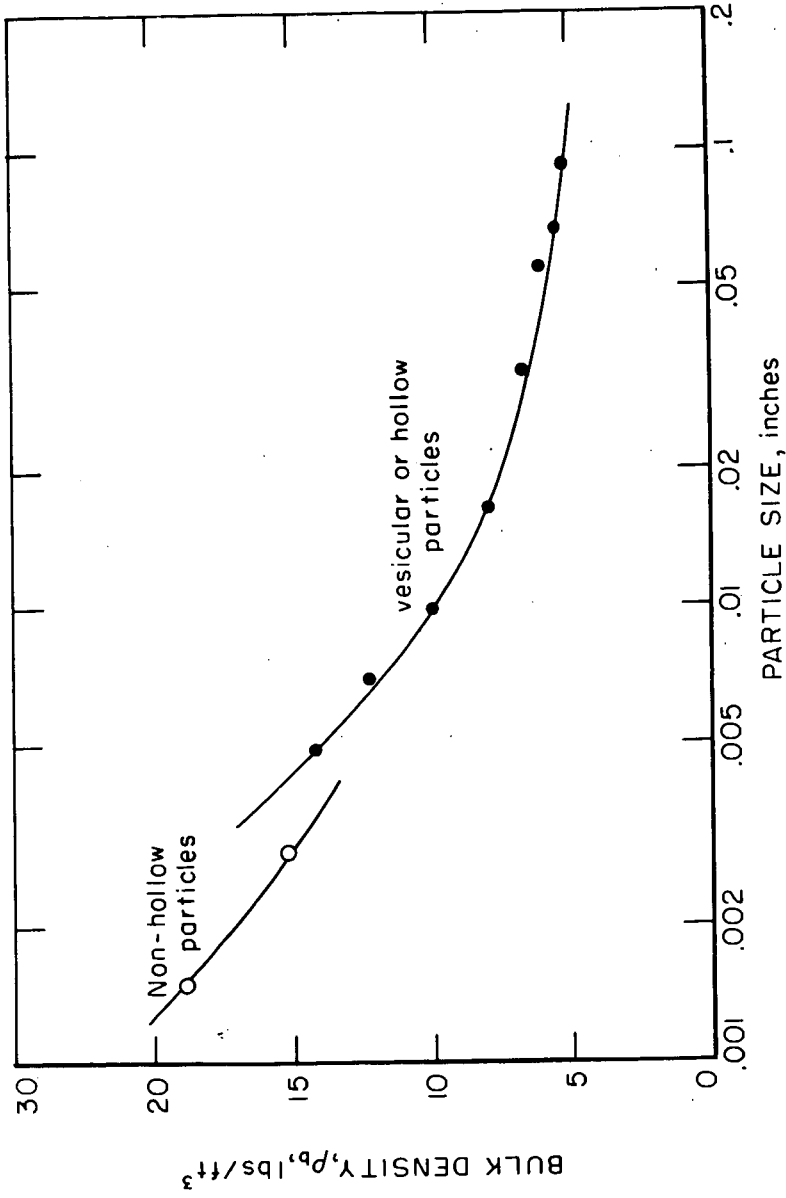


FIGURE 3.- Bulk Density vs Particle Size of Char.

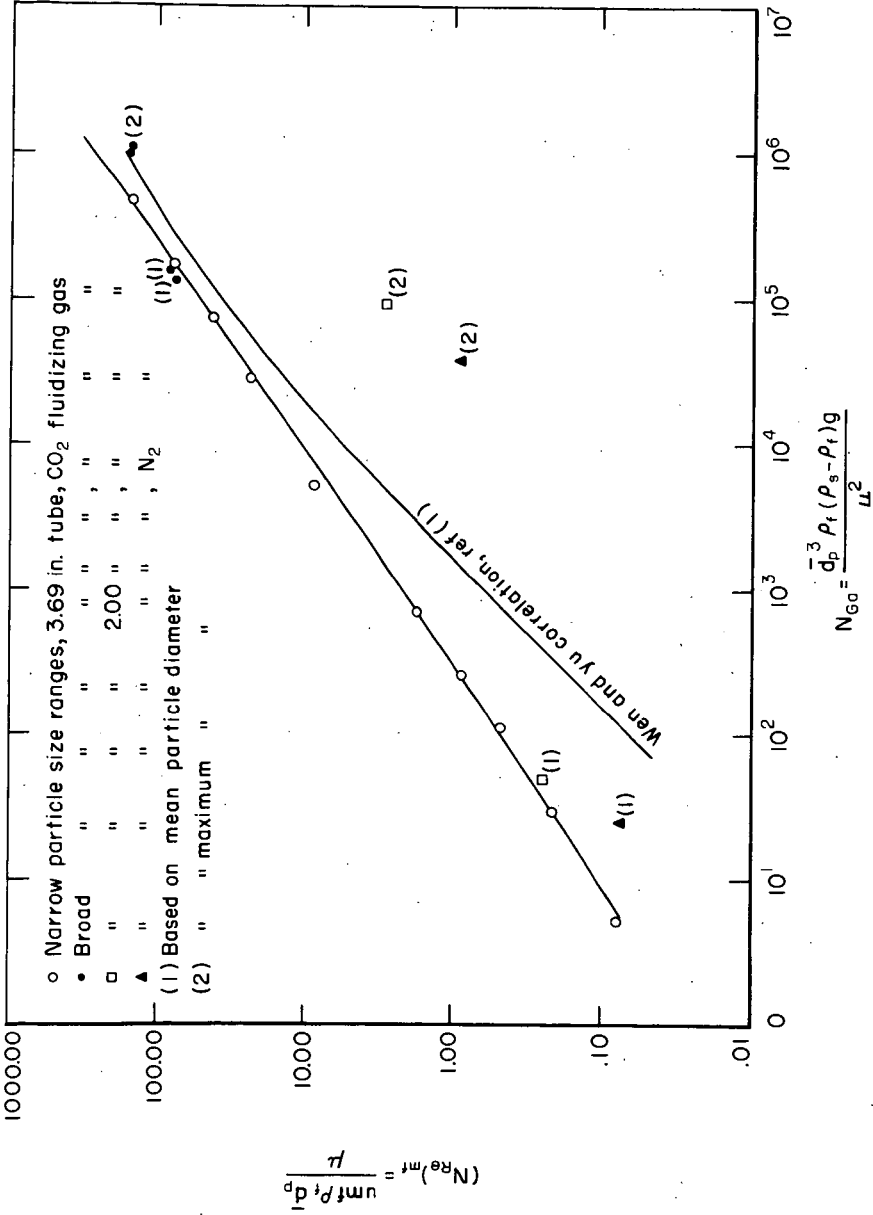


FIGURE 4.- Fluidization Correlation.

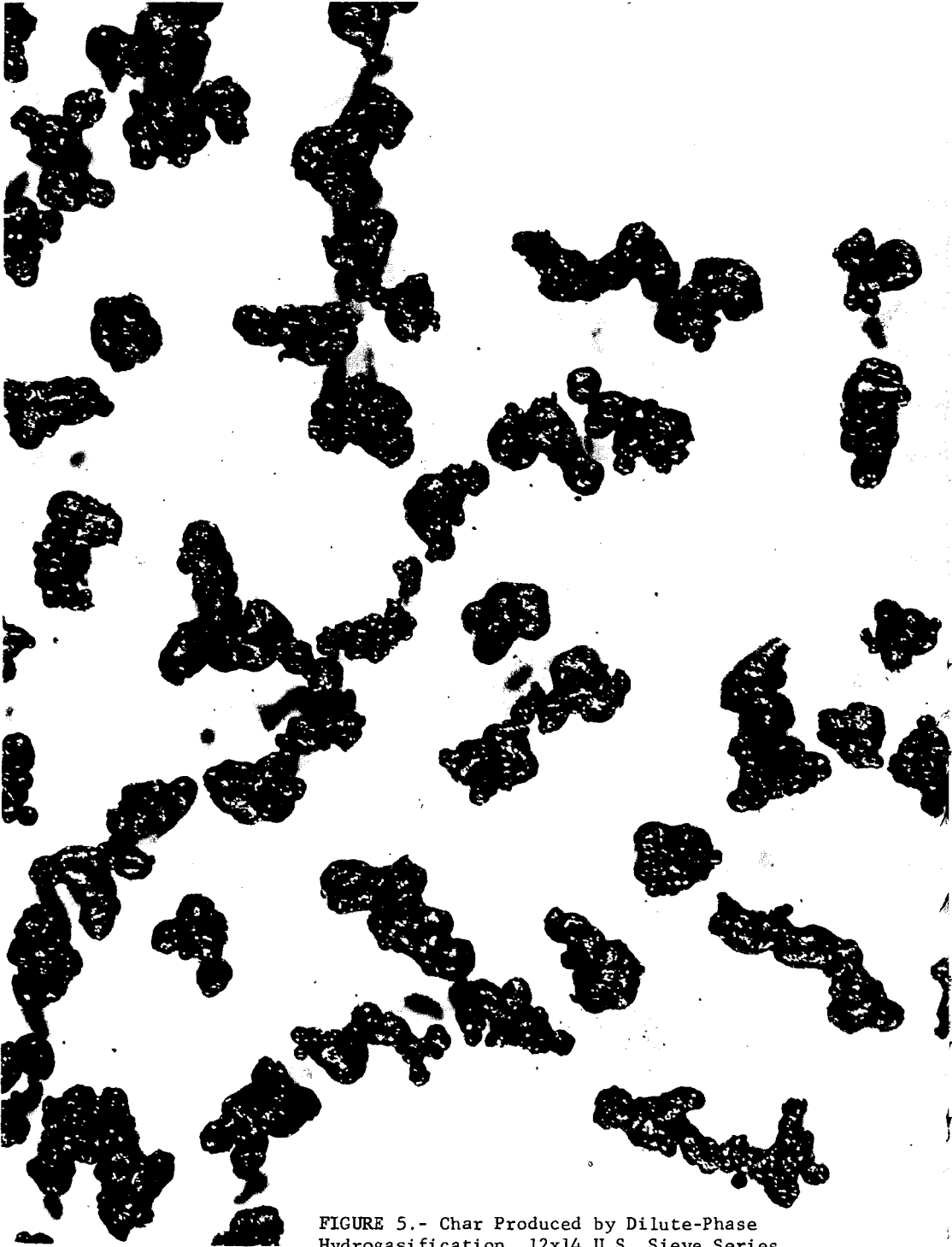


FIGURE 5.- Char Produced by Dilute-Phase Hydrogasification, 12x14 U.S. Sieve Series

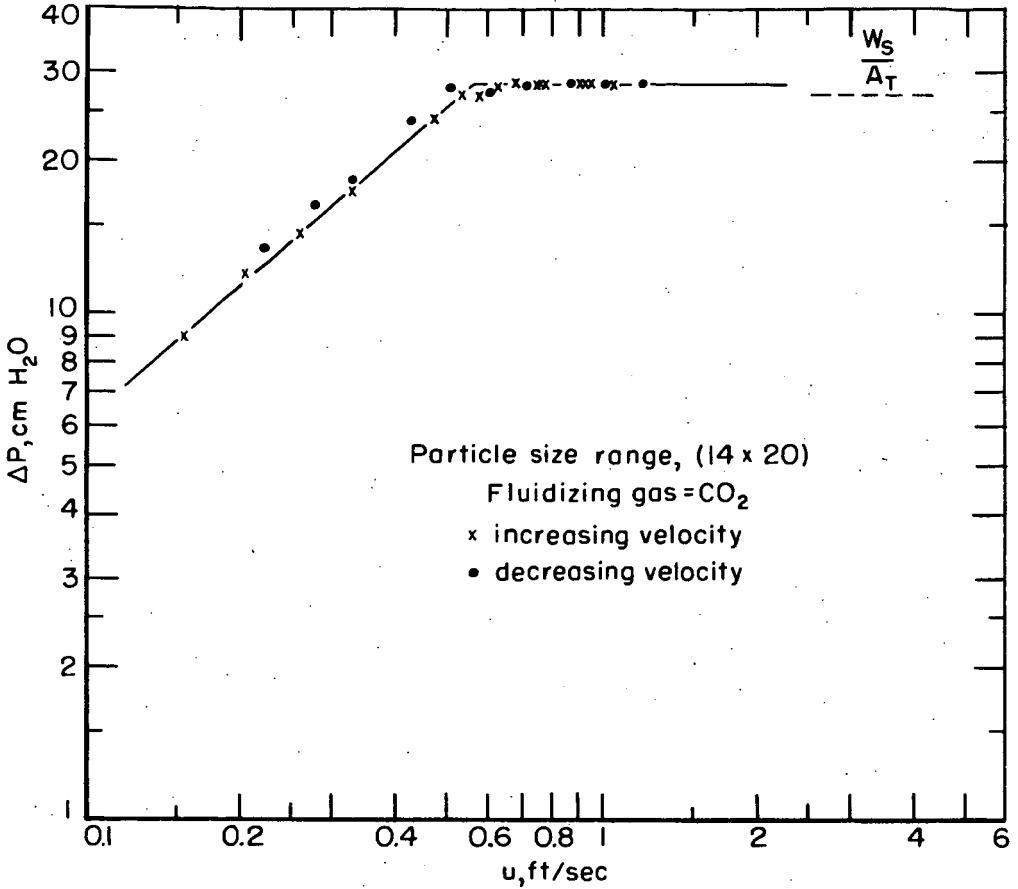


FIGURE 6a.- Typical Pressure Drop-Velocity Curve,
Narrow Particle Size Range..

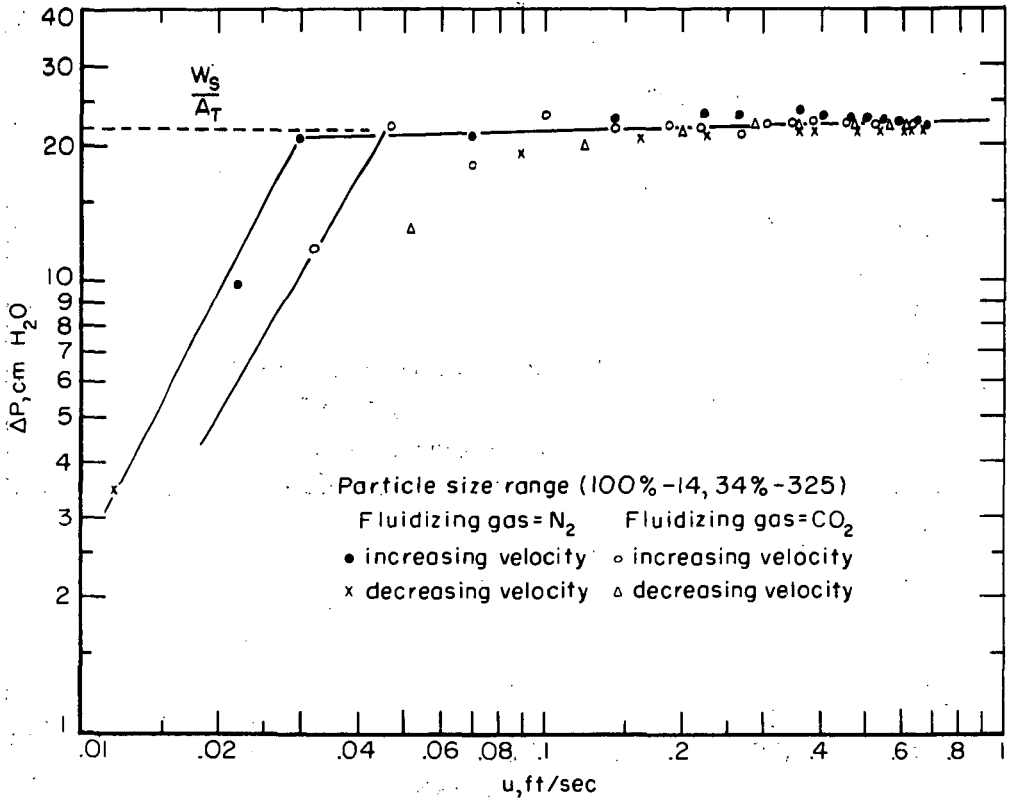


FIGURE 6b.- Typical Pressure Drop-Velocity Curve, Broad Particle Size Range.

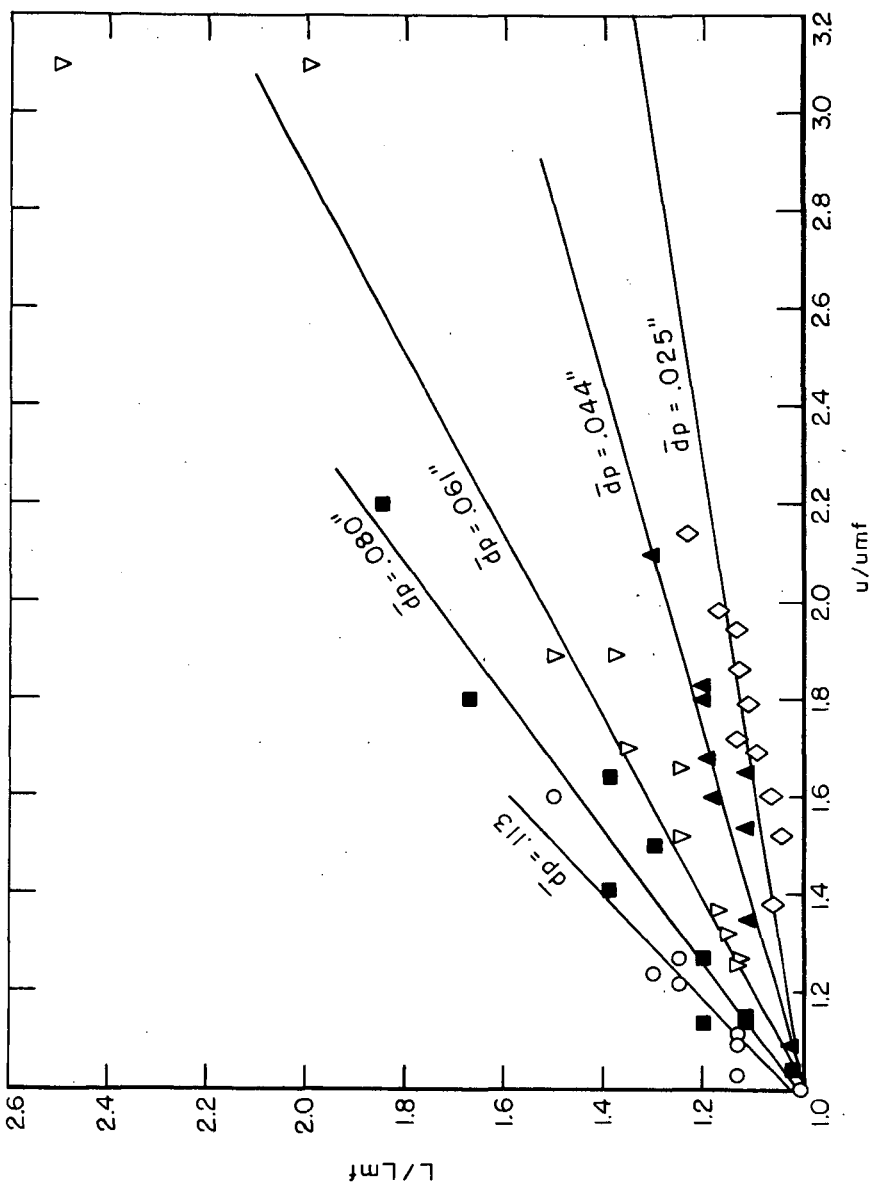


FIGURE 7a.- Effect of \bar{d}_p and u/U_{mf} on Bed Expansion.

L-12235

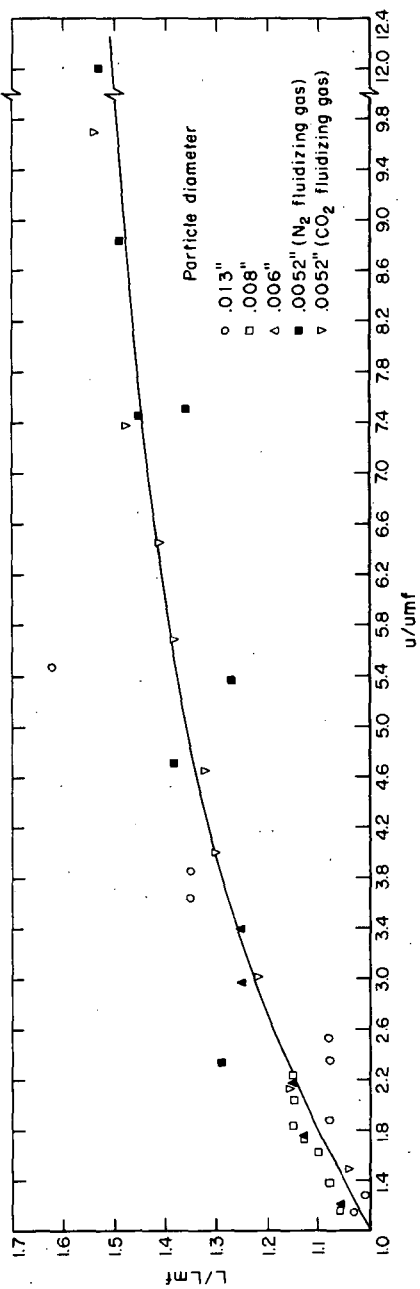


FIGURE 7b.- Effect of u/U_{mf} on Bed Expansion for $\bar{p} < .025$.

STUDIES ON THE PRODUCTION OF CARBON BLACK FROM COAL

M.S. Iyengar, R. Haque, R. K. Chakrabarti and M. L. Dutta

Regional Research Laboratory, Jorhat,
(Assam), India

ABSTRACT

Earlier work revealed that high volatile, vitrain rich and low ash coals could be converted to carbon black equivalent to thermal grade carbon black of commerce. In the present paper which is an extension of the earlier work some other coals have been used. It has been shown that by changing the reactor design and reaction variables the carbon black obtained is found to have properties of rubber and tyre grade products. Properties and compounding tests of the carbon black in rubber mix have been carried out and compared with those of standard products. A cost economics of the carbon black obtained from coal has also been discussed.

Coal has traditionally been used as fuels and there are very few studies describing the nonfuel use of coals. Johnson and co-workers (1,2) were the first to report on the conversion of high volatile coals into thermal black. They obtained the black as a byproduct in the production of hydrocyanic acid from coal. In an earlier paper (3) the present authors have described the production of thermal black from Assam coal. They adopted a transport reactor very much different to that used by the earlier workers and their main product was carbon black.

But thermal blacks find very limited use. The major demand is for rubber grade black for use in the tyre industry. The present paper describes studies on obtaining improved grades of carbon black from three bituminous coals of India. The paper also describes the techno-economic aspects of producing carbon black from coals.

Equipment and the process:

While the apparatus in the present studies are similar to that described earlier (3), the reactor, however, was designed to handle 70 lb./hour of coal. The inner wall of the reactor was made of 9 in. thick high alumina bricks followed by a 6 in. layer of insulation brick followed by a K.S. sheet. The reactor was 12 ft. high and 1 ft. in diameter.

A typical run was carried out as follows:-

Crushed coal (40 per cent through 200 BS) fed to the reactor through a rotary feeder is conveyed through the transport reactor by the carrier gas air. The reactor is initially heated to 500 - 600°C by burning low ash firewood. When the temperature becomes steady at the above temperature, the charging of coal is started. Partial combustion of the coal raises the temperature to 1300°C maximum. The air to coal ratio of the charges is kept constant at 65 cu.ft./lb. and the time of residence of the coal particles in the reactor is about 1.3 seconds. The carbon black is collected in the temperature range of 1200 - 1300°C. The char is separated from carbon black in a stainless steel cyclone separator. The carbon is recovered by first scrubbing it with water in the scrubber and then by electrostatic precipitation.

The product is then pelletised and dried at 400 - 450°C. Strict control of air/coal ratio and feed rate are important as changes may lead to existence of uncracked tar in the carbon black and deteriorate its property or lead to excessive combustion and give lower yield of the product. Figure 1 shows the unit for producing carbon black from coal.

Experimental results and discussion -

The work was carried out with three different coals of India formed under widely varying geological conditions. Table I shows the analysis of the coals used in the study.

Though they are all high volatile low rank coals, they differ in their caking characteristics and ash content. Sulphur content of the third coal is much lower than the two other coals. Reaction conditions were maintained identical and average test result of two or three runs has been shown. Table II shows the analysis of carbon blacks.

Figure 2 shows that the yield of carbon black bears a direct relationship with the hydrogen content of the coal. The Russians also obtained such relations (4), but details of their process are not available. The formation of carbon black from coal initially involves decomposition of coal to tar and gaseous hydrocarbons which ultimately undergoes dehydrogenation and aggregation to form carbon black. Theories on the carbon black formation differ mainly in the route and order in which these two essential changes occur (5).

Coals containing high mineral matter give a higher ash in the product. Consequently compounding tests have been carried out with only low ash carbon black produced from Baragolai colliery coal, Upper Assam. Figure 3 shows the electron micrographs of carbon black produced from Baragolai colliery coal (a) and HAF black(b). The study was carried out using a magnification of 52700 to determine the average particle size and the structure of the black. It is observed that carbon black obtained from coal is of high structure and is different from thermal black, which is also supported by its compounding test. The size of these particles varies from 200 - 800° A comparable with HAF blacks having particle size varying between 200 - 800°A. However, the frequency of distribution of bigger particles in the HAF black is much less than those in carbon black prepared from coal.

Figure 4 shows the x-ray pattern of carbon blacks obtained from (1) Baragolai colliery coal, (2) Pench Valley coal, and (3) Standard Sample HAF. It may be observed that the carbon blacks obtained from coals show bands of mineral matters, especially quartz, which is more prominent in the case of sample 2 obtained from Pench Valley coal containing higher percentage of mineral matter. The carbon band of samples 1 and 2 differ in intensity from that of number 3 as the formation of the latter takes place at temperature higher than those of 1 and 2. This may be attributed to the randomness in the degree of orientation of carbon particles in samples 1 and 2 whose formation takes place at lower temperature than that of sample 3.

Properties of the carbon black obtained from Baragolai colliery coal, Assam have been compared with two commercial carbon blacks in Table III.

Acetone extract which indicates the presence of uncracked tar in the product is slightly higher than those of the standard blacks. Iodine absorption values are greater than even HAF blacks. Surface area has been calculated from iodine absorption values (6), using the relationship $SDd = 60,000$, where S = surface area, D = density, d = particle size. D.B.P. absorption is very nearly equal to the HAF blacks but greater than the SRF blacks. pH of the product is in the mild acidic range which may be attributed to the nature of starting material.

Table IV shows the physical properties of rubber compounded with carbon black obtained from Barapalai colliery coal and compared with those compounded with a standard SRF black. Mooney viscosity which is an important property of the polymer mix is dependant mainly on the carbon black structure and loading in most polymers. In a 50 phr sample Mooney viscosity @ 100°C is found to be higher than the SRF blacks and Mooney scorch time about 0.64 times that of SRF blacks.

Rate of cure of the compound loaded with carbon black derived from coal is faster than compounds loaded with SRF blacks.

Physical properties like tensile strength, elongation at break and 300% modulus of the compound loaded with carbon black from coal are in line with SRF blacks, which shows it can substitute SRF blacks.

Cost economics:

A cost study of carbon black produced from coal revealed that the cost of production is \$ 70 per ton on the basis of 20 per cent conversion of coal to carbon black and price of coal being taken \$ 7.5 per ton. The price of char produced in the process (about 30 per cent) is taken as \$ 10.00 per ton. This is quite promising as the market price of carbon black in India varies from \$ 225 - 325 per ton.

Conclusion -

By changing the design and material of construction and altering the reaction variables the quality of the carbon black obtained from coal can be considerably improved to approach those of the rubber grade product. Some of the properties are similar to those of HAF. Though the physical properties like tensile strength, elongation at break and 300 per cent modulus of the compound loaded with carbon black from coal are lower than the compounds loaded with HAF blacks, they are in line with the SRF blacks. Experiments are still underway to produce HAF black.

Acknowledgement:

Grateful acknowledgement is made to M/s Synthetics and Chemicals Limited, Bombay and National Physical Laboratory, New Delhi for assistance and co-operation.

Literature Cited:

1. Johnson, G.E., Decker, W.A., Forney, A.J., Field, J.H. 158th National Meeting of American Chemical Soc. Division of Fuel Chemistry, New York, Sept. 7 - 12, 1969, Vol. 13, No. 3, pp.207-222.
2. Johnson, G.E., Decker, W.A., Forney, A.J., Field W.H. Rubber World, 156(3), 63-68, 1967.
3. Haque, R., Chakrabarti, R.K., Dutta, M.L., Iyengar, M.S. Sent for publication in J. Ind. Eng. Chem. R & D Section (under review).
4. Mischenko, M.L., Bagdanov, I.F., Farberov, I.L., Urkovski, I.M., Gilyazetdinov, L.P., Gugaev, B.I. Khim, Tverd. Topl., (2), 139-141 (Mar-Apr., 1969).
5. Gaydon, A.G., "The Spectroscopy of flames". Chapman & Hall Ltd., London, 1957, p. 189.
6. Smith, W.R., Thornhill, F.S., Bray, R.I., Ind. Eng. Chem. Indust., 33, 1303 (1941).

Table I - Analysis of the coals used for production of carbon black.

Details of the coals	Ash %	Moisture %	IV.M. % {DAF	Fixed Carbon % {	IC % {	H % {	S % {	N+O by diff. % {DAF	Caking properties
1. Baragolai colliery, Upper Assam	2.7	1.8	42.3	57.7	81.4	5.6	2.5	10.5	Highly caking.
2. Garo Hill, Lower Assam	6.5	1.4	49.5	50.5	80.3	5.8	2.5	11.4	Weakly caking.
3. Pench valley, M.P.	23.4	4.5	35.0	65.0	82.5	5.2	0.7	11.6	Non-caking.

Table II - Analysis of carbon blacks produced from different coals under reaction conditions.

Coal feed rate - 70 lb./hr.

Air/coal ratio - 65 cu. ft./lb.

Temperature range of collection of carbon black - 1200 - 1300°C.

Carbon black obtained from	Yield %	Ash %	Moisture %	V.M. %	F.C. %	C %	H %	S %	N+O (by diff.) %
1. Baragolai colliery, Upper Assam.	20	1.3	2.0	2.2	94.5	95.8	0.7	1.6	1.9
2. Garo Hill, Lower Assam.	22	4.2	2.5	2.6	90.7	95.4	0.8	1.7	2.1
3. Pench Valley, M.P.	14.4	18.3	1.4	3.8	76.5	94.7	0.7	0.4	4.1

Table III - Properties of carbon black obtained from Assam coal compared with those of commercial carbon black.

Carbon black obtained from	Acetone extract %	Iodine absorption values mg./g.	D.B.P. absorption values ml/100g.	Particle size, °A	Surface area M ² /g.	pH
1. Baragolai colliery coal, Upper Assam.	1.9	89	106	200 - 800	68	6.5 to 7.0
2. SRF black	0.4	30	70 - 80	600 - 800	25 - 30	6.0 - 6.5
3. HAF black	0.5	82	103±6	200 - 800	74 - 100	8.0 - 9.0

Table IV - Physical properties of rubber compounded with
*ACB and SRF.

Compound No.	50 phr SRF	50 phr ACB sample	60 phr ACB sample	70 phr ACB sample								
Mooney viscosity (ML4) @ 100°C	63.5	74.5	82.0	95.5								
Mooney scorch (MS) Time @ 127°C.	32'-43"	21'-30"	20'-25"	18'-30"								
Cure Index (RC) @ 127°C	6'-0"	5'-0"	4'-40"	4'-30"								
Time of cure @ 145°C	15' 25'	15' 35'	15' 25'	15' 25' 35'								
Tensile strength lb./sq. ft.	2946	3060	2960	2803	2817	2789	2960	2760	2660	2617	2560	
Elongation at break %	670	396	385	530	400	400	500	385	350	400	300	290
300% Modulus lb./cu.ft.	1217	2174	2230	1459	1945	1973	1730	2160	2274	2074	2560	-
Shore hardness A2	61	65	65	68	70	70	70	71	71	77	79	79

*ACB indicates carbon black obtained from Baragolai colliery coal, Upper Assam.

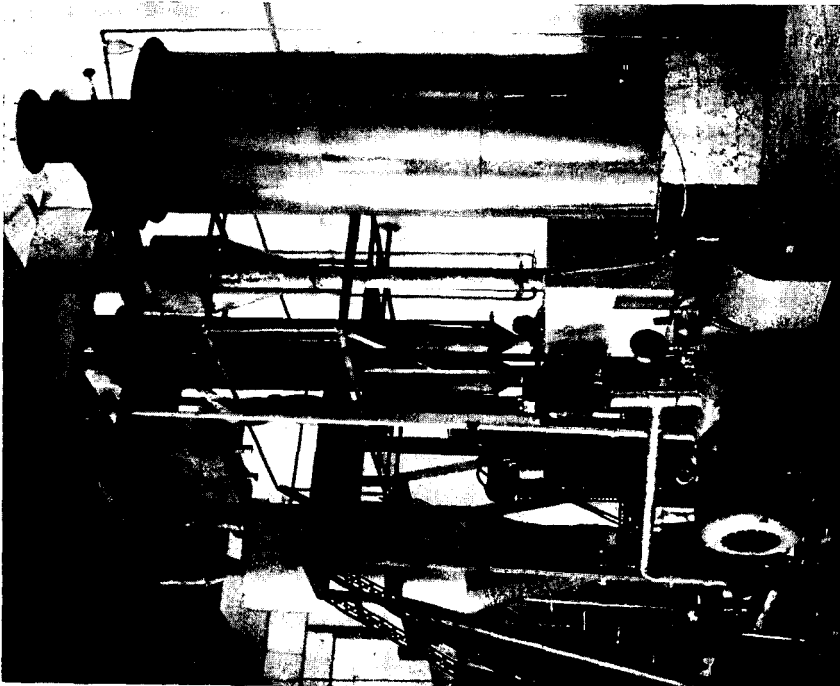


Figure 1. The unit for the production of carbon black from coal.

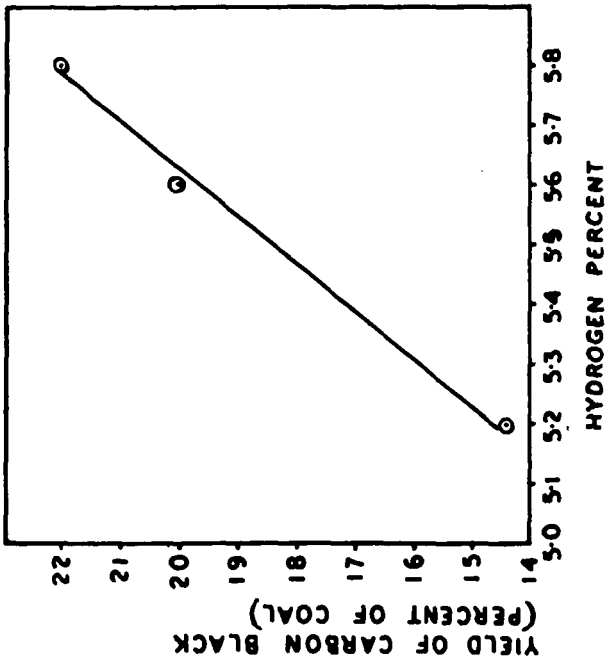


FIGURE - 2. RELATIONSHIP BETWEEN HYDROGEN CONTENT OF COAL AND YIELD OF CARBON BLACK FROM IT.

Figure 2. Relationship between hydrogen content of coal and yield of carbon black from it.

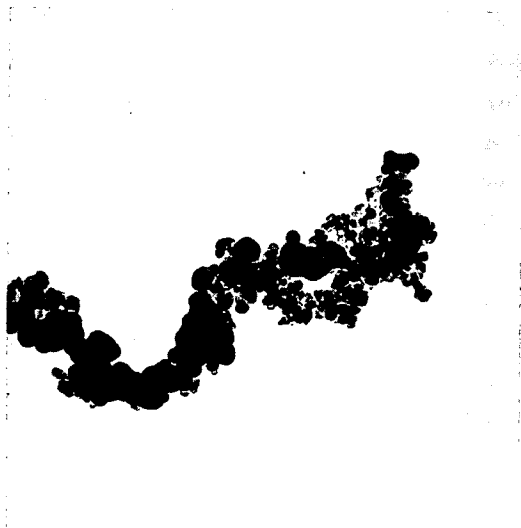
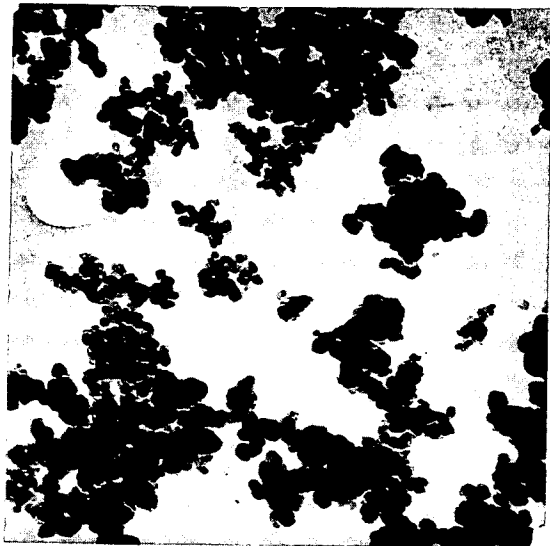
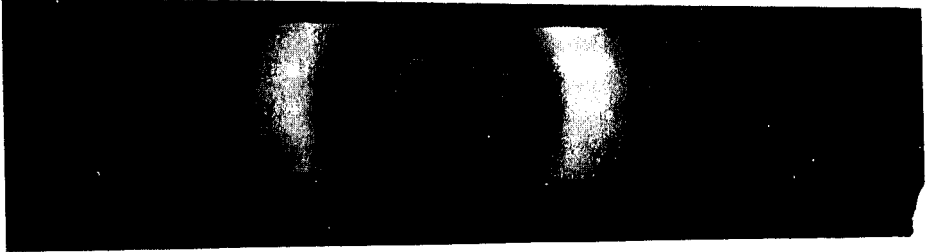
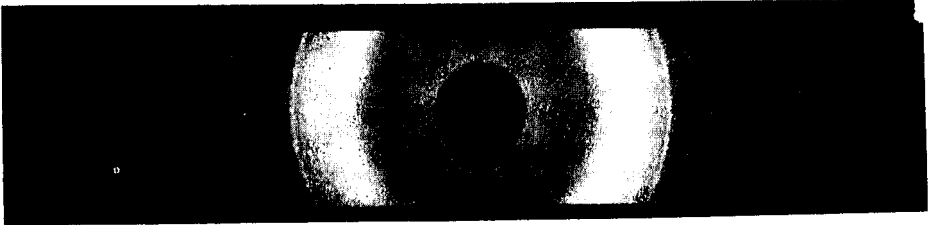


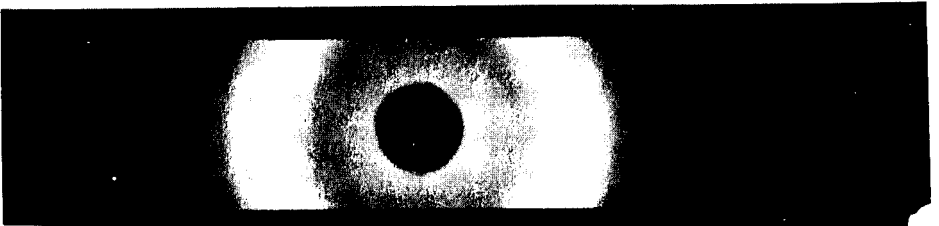
Figure 3. Electron micrograph of carbon blacks produced from (a) Paragolai colliery coal, Upper Assam, (b) HAF black (magnification 52700 times).



(1)



(2)



(3)

Figure 4. X-ray diffraction patterns of the carbon blacks obtained from (1) Baragolai colliery coal, Upper Assam (2) Pench Valley coal, M.P., (3) HAF black.